phys. stat. sol. (a) **53**, 433 (1979)

Subject classifications: 1.5 and 10.2; 22.1.1

Institute of Semiconductor Physics,
Academy of Sciences of the USSR, Siberian Branch, Novosibirsk

Dislocations and Stresses in a Crystal with an Island Film

By
E. M. TRUKHANOV, S. I. STENIN, and A. G. NOSKOV

Stresses and dislocations in substrate layers near the surface covered with rectangular islands of the film are analyzed. The characteristic features of equilibrium dislocation configurations are found. The major formulae are considered to estimate the shear and normal stresses in a substrate by equilibrium dislocation configurations. For systems as germanium–Si_3N_4 or –Si_3N_4 + SiO_2 films the stress levels due to Si_3N_4 densification at 800 °C heat treatment are determined. The effect of Ga diffusion into areas of the free substrate surface on the dislocation appearance is discussed.

На качественном уровне проанализированы напряжения и дислокации в приповерхностных слоях подложки, покрытой прямоугольными островками пленки. Определены признаки равновесных дислокационных конфигураций. Рассмотрены основные формулы, позволяющие по равновесным дислокационным конфигурациям оценивать сдвиговые и нормальные напряжения в подложке. Для системы германий–пленка Si_3N_4 или пленка Si_3N_4 + SiO_2 определены уровни напряжений, обусловленных уплотнением Si_3N_4 при термообработке 800 °C. Обсуждается влияние диффузии Ga в открытые участки подложки на появление дислокаций.

1. Introduction

Semiconductor–island dielectric film structures are widely used in microelectronics. Near the islands there arise stresses [1, 2] due to the misalignment of the thermal expansion coefficients of film and substrate, to the diffusion into free parts of the substrate surface, as well as to the film densification especially marked in pyrolitic dielectrics. These stresses can cause the appearance of dislocations [3 to 7]. Since a correct theoretical analysis of stresses in these systems is difficult, the latter can be estimated by equilibrium dislocation configurations as it has been done for continuous film structures (cf. [6], p. 222, and [7]). The present paper deals with dislocation configurations arising beneath islands of a simple form, and with estimating stresses in the system.

2. A Qualitative Analysis

Here a distribution of normal and displaced stresses in a crystal area adjacent to the film–substrate interface and the analysis of the shape of equilibrium dislocation configurations near the film islands are given.

2.1 Stresses in a crystal

We consider the stresses in layers parallel to the interface and placed at small but non-zero distance from it. We confine ourselves only to the case of the tensile film since for the compressed one the considerations are similar. Suppose that the smallest size of an island in the film plane ($x0y$) be many times greater than its thickness. Then the compressing normal stresses under the central part of the islands 1 to 3 (Fig. 1a) $\sigma_{xx} \approx \sigma_{yy}$ and are independent of coordinates x and y (Fig. 1b). Under the unclosed part of the crystal surface to the left of the island 1 σ_{xx} has a maximum near the edge of the island and tends to zero with distance. For some islands a superposi-

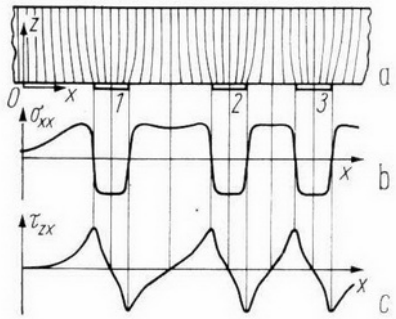

Fig. 1. Stresses in the substrate near the interface with film islands 1 to 3

tion of σ_{xx} takes place (Fig. 1 b). With increasing distance from the interface inside a substrate σ_{xx} decreases and becomes zero on the neutral surface. The latter is due to the fact that the island film bends the substrate in a similar way as a continuous film of less thickness.

The dependence of shear stresses τ_{zx} on x (Fig. 1 c) follows from the consideration of a bend of atomic planes normal to the interface (Fig. 1 a). Under the central part of islands and open areas of the crystal surface there is no bend and $\tau_{zx} = 0$, and near the edges the bend and τ_{zx} are extreme. A similar distribution of τ_{zx} was considered in [8].

2.2 Equilibrium dislocation configurations

In a homogeneous field of stresses a dislocation loop with size greater than the critical one unlimitedly expands. In case of an inhomogeneous field a dislocation may have an equilibrium position. If Peierls stresses are neglected, then with equilibrium $dE = dA$, where dE is the variation of dislocation energy and dA is the work in the field of stresses at infinitely small dislocation displacement. One can show that this equality is equivalent to the known expression

$$\tau_b = \frac{E}{bR}, \tag{1}$$

where τ_b is the shear stress along the slip direction, $\boldsymbol{b}$ the Burgers vector, and R the radius of dislocation curvature. Consider the equilibrium configurations near the square and rectangular islands of the film. We begin our analysis with the isolated square island ABCD (Fig. 2 a). The slip plane of the dislocation ($x0y$) is parallel to the interface and close to it. Near the island edges shear stresses are extreme (Fig. 1 c), therefore it is more likely that the dislocations arise there. τ_{zx} and τ_{zy} are equal to zero on the intercepts of EF and GH, respectively. Thus, on EF $\tau_b = 0$ for $\boldsymbol{b}_1 \parallel \overrightarrow{SG}$. Further such lines will be called the lines $\tau_b = 0$. The loop 1 coincides with the central part EF, surrounds the part of square where $\boldsymbol{\tau} \cdot \boldsymbol{b} > 0$ (vector $\boldsymbol{\tau} = \tau_{zx}\boldsymbol{i} + \tau_{zy}\boldsymbol{j}$), and because of linear tension does not pass through points E and F. For loop 2 ($\boldsymbol{b}_2 \parallel \overrightarrow{SA}$), line $\tau_b = 0$ is the diagonal BD. The loop with $\boldsymbol{b}$ direction between $\boldsymbol{b}_1$ and $\boldsymbol{b}_2$ occupies an intermediate position. Taking account of the fact that the square has a fourth-order axis, the equilibrium form of the dislocation loop with arbitrary $\boldsymbol{b}$ can be represented.

Now we consider the equilibrium dislocation loops arising near islands of elongated rectangular shape. At the points which are removed from the short sides AD and BC (Fig. 2 b), $\tau_{zy} = 0$. Therefore, on the segment SS′, being at equal distances from AB and CD, $\boldsymbol{\tau} = \boldsymbol{0}$, and, consequently, SS′ will be involved into any equilibrium loop with $\boldsymbol{b}$ non-parallel to a short side of the island. Near the vertices of the rectangle, $\boldsymbol{\tau}$ are the same as near the vertices of the square. Therefore, loop 2 in Fig. 2 a and the loop with similar $\boldsymbol{b}$ in Fig. 2 b have equal form near B and D. As Fig. 1 c shows, for adjacent islands the lines $\tau_b = 0$ arise not only inside the islands, but also between them. Fig. 2 c

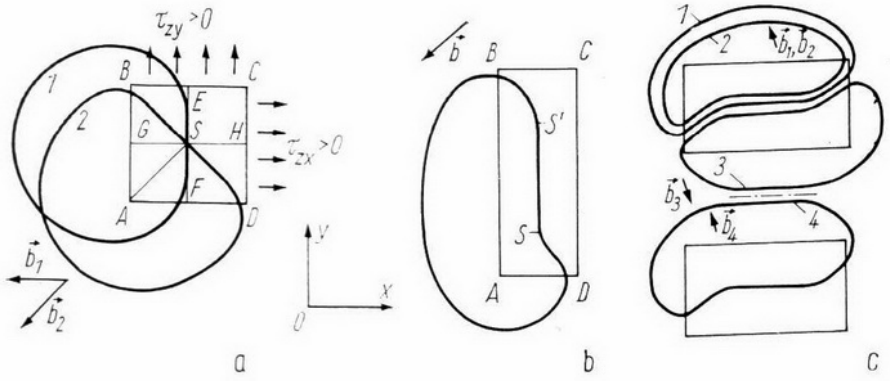

Fig. 2. Equilibrium configurations of dislocation loops under the film islands. a) Square island; b) rectangular island; c) interaction of dislocations under the rectangular islands

demonstrates loops 1 to 4 having a common slip plane and $\boldsymbol{b}_1 = \boldsymbol{b}_2 = \boldsymbol{b}_4 = -\boldsymbol{b}_3$. A distinguishing feature of the equilibrium of such loops is the symmetrical position of straight mutually repulsive dislocation intercepts relative to the line $\tau_b = 0$.

3. Results and Discussion

Ge (111) substrates of 0.5 mm thickness doped with Sb up to the concentration 6×10^{15} cm^{-3} were used. Two-layer films Si_3N_4 (1200 Å) + SiO_2 (500 Å) or films Si_3N_4 (1200 Å) were grown (see [6], p. 126). The temperatures of synthesis of Si_3N_4 and SiO_2 films were 800 and 670 °C, respectively.

3.1 Germanium dislocation structure

In crystals subjected to diffusion or annealing at the diffusion temperature no differences of the shapes of dislocation loops have been found, but after 0.5 and 5 h diffusion the fraction of islands with dislocations was 0.45 and 0.82, respectively, and after annealing it was only 0.13. In addition to this, after the diffusion the dislocation density near islands increased, too. For each regime 200 to 300 islands on the two wafers were examined.

Typical dislocation configurations shown in Fig. 3 have all the features usual for equilibrium. So, loops 1 and 2 in Fig. 3a and loops 1 to 3 in Fig. 3b have bends towards the D- or D_1-vertex due to the direction $\boldsymbol{b}$ (cf. Fig. 2b). When the depth of loop location increases, such bends disappear, as decreasing $\boldsymbol{\tau}$ results in loop contraction. The straight segments of loops 1 and 2 in Fig. 3a are at the centre of the island and at the open area of the substrate (cf. Fig. 2c), but each one of the loops 1, 2 and of the loop 3 in Fig. 3b is displaced from the centres. This displacement will be used further for the determination of σ_{xx}.

The main complication of loop shapes is their discontinuity due to the two effects. The first is connected with the exit of screw segments on the surface by means of cross-slip. Fig. 3c shows a group of loops produced by the same source. As the diffraction analysis showed, the exits of dislocations on the crystal surface (see area marked by I) lie along a line parallel to $\boldsymbol{b}$, showing that the screw segments of all the loops have cross-slipped along the same plane. The exits of loops 1, 2 (Fig. 3a) and 4 (Fig. 3b) are also due to cross-slip, dislocation segments affected by linear tension near the exits being displaced toward the island edges against the external stress field τ_{zx}.

The second reason of loop discontinuity consists in the non-parallel alignment of (111) and the substrate surface. Fig. 3b shows two groups of dislocations having passed out of the crystal on the surface along the traces (AB and A_1B_1) of the slip plane (111). Each of these dislocations displaces the substrate relative to the film by $\boldsymbol{b}$, which is the cause of the elastic displacement of Ge and the black–white contrast on lines AB and A_1B_1. Earlier (cf. [6], p. 222 and [7]) step images at the interface Ge–SiO_2 (con-

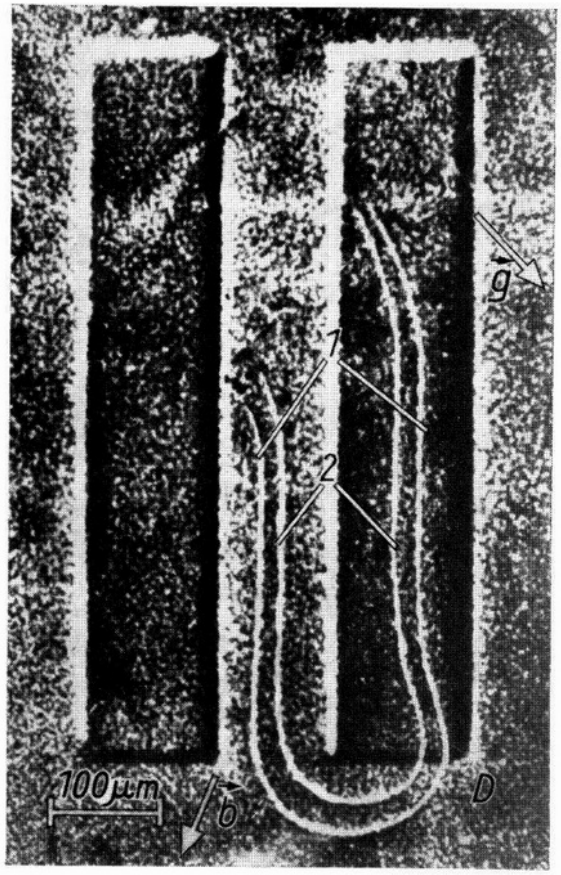

a

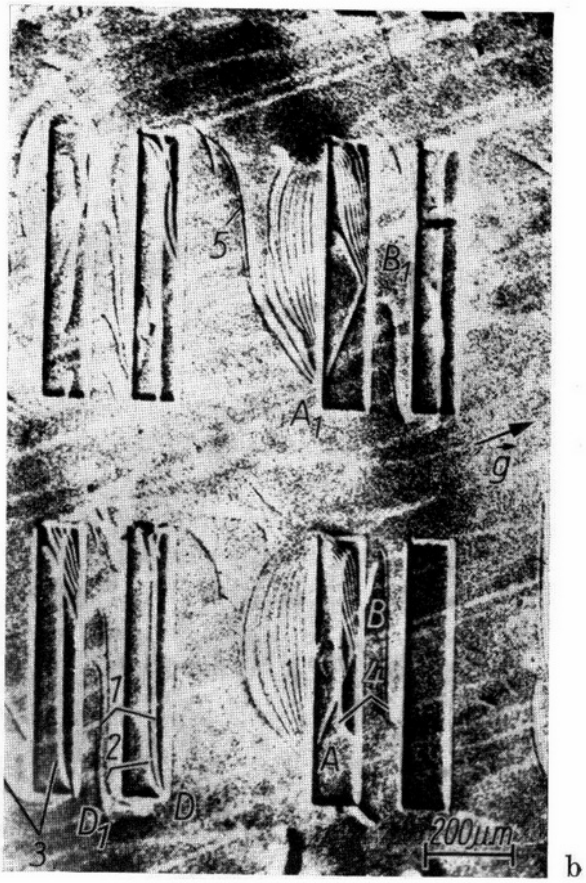

b

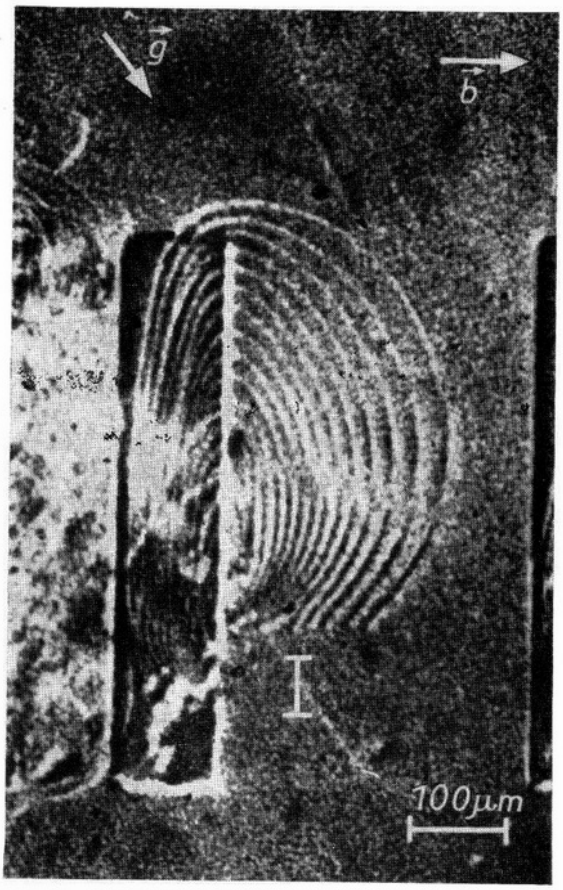

c

Fig. 3. Typical forms of dislocation loops; $\boldsymbol{g} = [\bar{2}20]$. a) After annealing; b) and c) after 5 h diffusion

tinuous film) were observed by X-ray topography for dislocations gliding on inclined {111}. As in the cross-slip situation the linear tension displaces the dislocation ends against the external stress field towards the points B and B_1. We think that variations of the loop form affected by linear tension near the line $\tau_b = 0$ are additional evidence of the equilibrium configuration.

Note that loop 5 interacted with the dislocation glide on the tilted plane {111} and reached an adjacent island. The dislocation interaction is not considered in the paper, but it is interesting that the sign and radius of curvature of loop 5 between the islands qualitatively corresponds to the sign and the value of the field τ_{zx}.

3.2 Estimation of stresses

3.2.1 Stress determination from equilibrium pile-up of rectilinear dislocations

To find τ_{zx} and σ_{xx} in a crystal near the surface, we determine τ_b from the equilibrium conditions of rectilinear dislocations in a pile-up located close to the line $\tau_b = 0$ (Fig. 3 a, b). The above equilibrium of the rectilinear dislocation of the pile-up is achieved if

$$b\tau_b = P + P_{\text{im}}\,, \tag{2}$$

where P and P_{im} are forces of interaction with the rest of the pile-up dislocations and their images, respectively. For two dislocations with equal $\boldsymbol{b}$,

$$P = \frac{Gb^2}{4\pi r}\left(\frac{\sin^2\alpha}{1-\nu} + \cos^2\alpha\right), \tag{3}$$

where G is the shear modulus, ν the Poisson coefficient, α the angle between the dislocation line and $\boldsymbol{b}$, and $2r$ the distance between the dislocations. P_{im} can be more simply estimated if the image dislocations are placed in positions symmetrical to the initial dislocations relative to the crystal surface. The dislocation interaction with its own image can be neglected, since the slip plane makes a small angle with the surfac of the substrate. Then, for a case of two dislocations with equal $\boldsymbol{b}$ and a common slip plane,

$$P_{\text{im}} = \frac{Gb^2}{4\pi}\frac{r}{r^2+h^2}\left(\frac{\sin^2\alpha}{1-\nu}\frac{r^2-h^2}{r^2+h^2} + \cos^2\alpha\right), \tag{4}$$

where h is the depth of the dislocation position. When analysing the pile-ups containing three and more dislocations, P and P_{im} have several elements computed by (3) and (4).

The quantity τ_b defined by (2) to (4) can be expressed, on the other hand, through the stress tensor $\boldsymbol{\sigma}$. Near the central part of rectangular islands $\tau_{zy} \approx 0$ and $\sigma_{xx} \approx \sigma_{yy}$; then $\sigma = \sigma_{xx}(\boldsymbol{ii} + \boldsymbol{jj}) + \tau_{zx}(\boldsymbol{ki} + \boldsymbol{ik})$. Everywhere in Section 3.2.1 the considerations given for the centres of islands are true also for those of open areas of the crystal surface. Let the angle between the planes $(x0y)$ and (111) be equal to φ, and the trace (111) in the $(x0y)$ plane make the angles β with $0x$ and γ with $\boldsymbol{b}$. If the unit vectors along [111] and $\boldsymbol{b}$ are denoted through $\boldsymbol{e}_{111}$ and $\boldsymbol{e}_b$, then $\tau_b = (\boldsymbol{\sigma e}_{111}) \cdot \boldsymbol{e}_b$, and with small φ,

$$\tau_b = \tau_{zx}\cos(\beta+\gamma) - \sigma_{xx}\varphi\sin\gamma\,. \tag{5}$$

It is seen that with $\varphi = 0$ or $\gamma = 0$,

$$\tau_b = \tau_{zx}\cos(\beta+\gamma)\,, \tag{6}$$

$(\beta + \gamma)$ being the angle between $0x$ and $\boldsymbol{b}$. Here $\tau_b = 0$ in the centre of the island, where $\tau_{zx} = 0$ (Fig. 1 c). When φ and γ are not equal to zero, line $\tau_b = 0$ is not situated in the centre of the island. Fig. 3 b illustrates the displacement of rectilinear intercepts of dislocation loops from centres of islands and open areas of the substrate. τ_{zx} and σ_{xx} can be found by the known value τ_b if in the centre of the island τ_{zx} is taken linear in x and $\sigma_{xx} = \text{const}$. We choose the origin of coordinates to be in the island centre (Fig. 4 a). According to (5) τ_b is also linear in x near the origin (Fig. 4 b). With some $x = x_0$ the stress $\tau_b = 0$; therefore, the two dislocations (e.g., 1 and 2 in Fig. 3 b) lie at the points $x_0 \pm r$ (Fig. 4 a). Using equations (2) to (4). one can determine from the experiment the

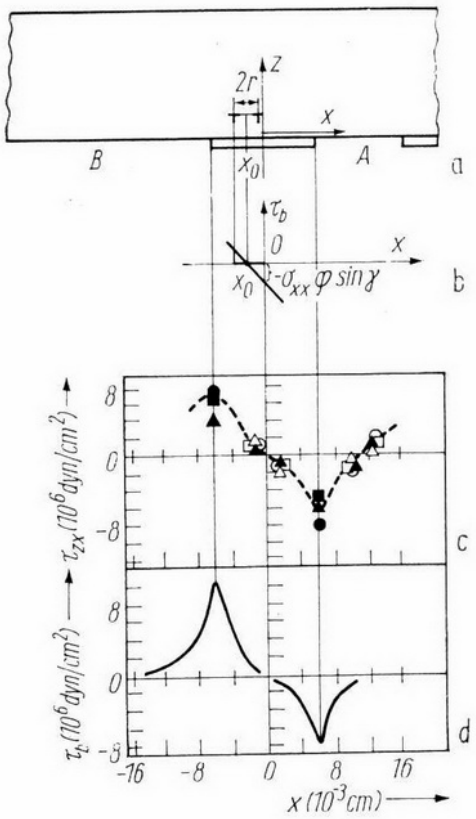

Fig. 4. Experimental determination of shear stresses: a) Equilibrium positions of dislocations near the displaced line $\tau_b = 0$. b) Assumed dependence of τ_b vs. x in the central part of the island. c) The mean value of τ_{zx}: ○, ● 5 h annealing; □, ■ 0.5 h diffusion; △, ▲ 5 h diffusion; ○, □, △ τ_{zx} calculated from the action of the straight dislocations; ●, ■, ▲ τ_{zx} found from the curvature radius. A is the open area of 104 × 650 μm², B is the open area of 350 × 650 μm². d) Dependence of τ_b vs. x defined from the curvature radius of the dislocations

stresses $\tau_b(x_0 \pm r)$, then calculate τ_{xz} at the points $x = \pm r$. Really, according to (5) the lines $\tau_{zx}(x) \times$ $\times \cos(\beta + \gamma)$ and $\tau_b(x)$ make equal angles with the axis $0x$. As the first line passes through the origin and the second one through x_0, one can write

$$\tau_{zx}(\pm r) = \frac{\tau_b(x_0 \pm r)}{\cos(\beta + \gamma)}. \tag{7}$$

According to (5) $\tau_b = -\sigma_{xx}\varphi \sin\gamma$ at $x = 0$. From the similarity of the triangles located near the point x_0 (Fig. 4 b) it follows that

$$\sigma_{xx} = \frac{x_0 \tau_b(x_0 - r)}{r\varphi \sin\gamma}. \tag{8}$$

For an experimental determination of $\tau_b(x_0 \pm r)$ pile-ups of two or three dislocations were used. The loops having exits on the surface because of non-parallel alignment of (111) and ($x0y$) were analysed, since h is easily determined for them. The angle φ measured by an X-ray diffractometer was not greater than 3°, and h was 3 to 15 μm. The effect of the film on P_{im} [9] is neglected as the film thickness $t_f \ll h$. $\sigma_{xx} =$ $=$ (2 to 8) $\times 10^7$ dyn/cm², calculated by equation (8), have opposite signs, but about the same values for islands and open areas as they have nearly the same dimensions (120 × 650 and 104 × 650 μm²). Fig. 4 c shows τ_{zx} evaluated from (2) to (7). Both σ_{xx} and τ_{zx} are about the same for all treatments of specimens, both for one-layer and two-layer films. The accuracy of calculating τ_{zx} is about 50% since the account of P_{im} was simplified. Besides, the width of the dislocation image on the topographs is comparable with the distance between them. The accuracy of determining σ_{xx} is several times lower, since a wide image of the island edge does not allow an exact determination of x_0.

To make a rough estimate of the normal stresses in the island film, σ_f, we assume σ_{xx} in the substrate near the interface and far from the film edges to be equal in island film–substrate and continuous film–substrate structures, the other parameters being equal. If $\sigma_{xx} = 5 \times 10^7$ dyn/cm², then according to [10] $\sigma_f = \sigma_{xx} t_s / 4t_f = 5 \times 10^{10}$ dyn/cm², where t_s is the thickness of the substrate.

3.2.2 Determination of stresses from the curvature of the equilibrium dislocation loop

Formulas (2) to (4) and (1) allow to calculate τ_b by independent ways. To eliminate the influence of adjacent dislocations using (1), it is necessary to analyse single loops. The further account of τ_{xz} is possible only in centres of islands and uncoated areas using

(7), as well as at the film edges for which far from the short sides $\sigma = \tau_{zx}(\boldsymbol{ki} + \boldsymbol{ik})$ and (6) holds, though φ and γ are not zero. τ_{zx} estimated by (1), (7), and (1), (6) are shown in Fig. 4c. It is seen that calculations by (1), (7), and (2) to (7) give close results with comparable accuracy. The mean level of τ_{zx} at the edges of islands is 6×10^6 dyn/cm^2. Each of the values determined in any way is the result of three measurements on an average.

Fig. 4d shows the dependence $\tau_b(x)$ calculated by (1). Note that in some cases the loop intercepts lie along rectilinear Peierls valleys. These configurations have not been used for the calculations.

3.2.3 The main factor causing stresses

The calculated σ_{xx} and τ_{zx} are not due to diffusion since they do not depend on the conditions of specimen treatment. The other possible causes for stresses to arise are the dielectric densification (see [11], [6], p. 222, and [7]) and different thermal expansion coefficients of materials ($\alpha_{Ge} = 6 \times 10^{-6}$; $\alpha_{SiO_2} = 5 \times 10^{-7}$; $\alpha_{Si_3N_4} = 2.75 \times$ $\times 10^{-6}$ K^{-1} [12]). To determine the main cause we estimate the stresses in the film, σ_T, occurring due to cooling. In approaching an infinitely thick substrate, $\sigma_T = E_f(\alpha_f - \alpha_s)(T_0 - T_1)/(1 - \nu_f)$, where index „f" refers to the film and „s" to the substrate, T_1 is the temperature for which σ_T is calculated, and T_0 is the temperature of synthesis. For Si_3N_4 $T_0 = 800$ °C, for SiO_2 — 670 °C. If σ_f is taken to be caused by cooling, then T_1 is the minimum temperature (300 °C, [13]) at which dislocations in Ge can move at the distance recorded by X-ray topography. According to the calculation σ_T in a one-layer film and the average σ_T in a two-layer film are equal to 2.6×10^9 and 2.3×10^9 dyn/cm^2, respectively. As $\sigma_T \ll \sigma_f$, the stresses in the system are due to the densification, and no appreciable displacement of dislocations arises during the cooling of films. Islands of the film and free areas of the substrate are elongated, and the substrate under the islands is compressed. As σ_{xx} and τ_{zx} for one-layer and two-layer structures are equal, they arise mainly due to Si_3N_4 densification. The σ_f values obtained are in reasonable accordance with $\sigma_f = (1.2 \text{ to } 1.8) \times 10^{10}$ dyn/cm^2 in a continuous annealed film of Si_3N_4 on silicon [14] and is one order of magnitude greater than in a continuous pyrolitic SiO_2 film on Ge (see [6], p. 222, and [7]). An estimate of the volume densification of Si_3N_4 carried out in a way similar to [6, 7] for SiO_2 gives $\Delta V/V \approx 10\%$.

3.2.4 Peculiarities of the stressed state after diffusion

Diffusion causes more dislocations than annealing though the stresses at the depth of 3 to 15 μm as shown in Sections 3.2.1 and 3.2.2 are about equal. For discussing these facts let us compare the stresses on Ge due to dielectric densification and Ga diffusion (the Ga diffusion coefficient at 800 °C is 2×10^{-13} cm^2/s [15]). The strain of the diffusion layer, ε_d, is estimated in the approximation of an infinitely thick substrate since after 5 h diffusion from a constant source the p–n junction depth is ≈ 4 μm, that is 130 times less than the substrate thickness. Taking the Ga atoms to be non-compressed (evaluation of ε_d from the maximum), we have according to [16] $\varepsilon_d = 3[(1-\nu)/(1+\nu)] \times$ $\times [(r_s - r_d)/r_s]\,(n/n_0)$, where r_d and r_s are covalent radii of diffusing and matrix atoms, respectively ($r_d = 1.27$ Å, $r_s = 1.22$ Å), n and n_0 are the atomic numbers of diffusant and matrix in a unit volume, respectively. The compressing normal stresses due to diffusion are equal to $\sigma_d = \varepsilon_d E/(1 - \nu)$. Near the surface itself $n = 1.1 \times 10^{20}$ cm^{-3} and $\sigma_d = 3.6 \times 10^8$ dyn/cm^2, that is considerably higher than the tension stresses σ_{xx} under the open parts. However, already at the depth of 2 μm $n = 2 \times 10^{18}$ cm^{-3} and $\sigma_d = 5 \times 10^6$ dyn/cm^2. The estimate obtained explains the equal level of σ_{xx} at the depth of more than 3 μm in crystals after diffusion and annealing.

Now for substrate layers lying deeper than 3 μm we qualitatively compare τ_{zx} arising from the edges of the discontinuous diffusion layer and the dielectric layer. The signs of these stresses coincide. If thicknesses and elastic constants of the layers are equal, then the layer having higher normal stresses would cause the greater τ_{zx} in the substrate. Since the thicknesses t of the layers are not equal, we compute a normal distributed load q arising in the direction of x in cross-sections of the layers. The quantity $q_s = \sigma_f t_s$ of a dielectric film is 6×10^5 dyn/cm. The load of the diffusion layer, q_d, is computed by integrating the product of σ_d by the depth variation. The integration is performed within the thickness of a diffusion layer and gives $q_d = 2.4 \times 10^4$ dyn/cm, being almost completely within a 2 μm thick layer. As an estimation of ε_d was performed from the maximum, the real values of q_d are even lower. Though being approximate, the calculations done allow to understand why at depths greater than 3 μm the main role is played by τ_{zx} due to the edges of the dielectric film.

Returning to the question on the higher density of dislocations after diffusion, we note the two possible causes of this effect. First, a higher concentration of dislocation sources can exist in the diffusion layers. Second, near the surface one may suppose an increase of the fraction of τ_{zx} due to the diffusion layer.

4. Conclusions

In the present paper based on the analysis of dislocation configurations around islands of simple shape the normal and shear stresses in the substrate have been estimated. Note that for computing stresses in crystals a necessary condition is the equilibrium dislocation configuration. Consequently, to find stresses under the islands of more complex shape it is necessary to establish these configurations. The latter can exist for dislocations gliding in the plane which is nearly parallel to the interface.

Acknowledgements

The authors thank E. B. Gorokhov, Dr. K. K. Zilling, Dr. S. B. Pokrovskaya, Dr. I. G. Neizvestny for assistance in the work and helpful discussions, and G. A. Sokolova for specimen preparations.

References

[1] B. J. ALECK, J. appl. Mech. **16**, 118 (1949).
[2] K. A. VALIEV, B. I. KOZLOV, A. A. KOKIN, A. G. MALOV, and A. V. RAKOV, Mikroelektronika, Vol. 5, Izd. Sovietskoe Radio, Moskva 1972 (p. 282).
[3] J. A. BLECH, E. S. MEIERAN, and H. SELLO, Appl. Phys. Letters **7**, 176 (1965).
[4] V. M. TULUEVSKII, U. YA. ERTELIS, and I. A. FELTYNSH, Elektr. Tekh., Ser. 2, No. 8, 76 (1974).
[5] A. CERUTTI and C. GHEZZI, phys. stat. sol. (a) **17**, 237 (1973).
[6] A. V. RZHANOV (Ed.), Svoistva struktur metal–dielektrik–poluprovodnik, Izd. Nauka, Moskva 1976 (pp. 126 and 222).
[7] E. M. TRUKHANOV, E. B. GOROKHOV, and S. I. STENIN, phys. stat. sol. (a) **33**, 435 (1976).
[8] S. M. HU, S.P. KLEPNER, R.O. SCHWENKER, and D.K. SETO, J. appl. Phys. **47**, 4098 (1976).
[9] L. N. ALEKSANDROV and I. A. ENTIN, phys. stat. sol. (a) **27**, 665 (1975).
[10] R. J. JACCODINE and W. A. SCHLEGEL, J. appl. Phys. **37**, 2429 (1966).
[11] W. A. PLISKIN and H. S. LEHMANN, J. Electrochem. Soc. **112**, 1013 (1965).
[12] G. V. SAMSONOV, Nemetalicheskie nitridy, Izd. Metallurgy, Moskva 1969 (p. 174).
[13] J. R. PATEL and P. E. FREELAND, J. appl. Phys. **42**, 3298 (1971).
[14] M. TAMURA and H. SUNAMI, Japan. J. appl. Phys. **11**, 1097 (1972).
[15] V. M. GLAZOV and V. S. ZEMSKOV, Fiziko-khimicheskie osnovy legirovaniya poluprovodnikov, Izd. Nauka, Moskva 1967 (pp. 126 and 127).
[16] J. FRIEDEL, Phil. Mag. **46**, 514 (1955).

(Received May 26, 1978)